esa

ECOSPHERE

Patterns of tree mortality in a temperate deciduous forest derived from a large forest dynamics plot

Erika Gonzalez-Akre,[1] Victoria Meakem,[1] Cheng-Yin Eng,[1] Alan J. Tepley,[1] Norman A. Bourg,[2] William McShea,[1] Stuart J. Davies,[3,4] and Kristina Anderson-Teixeira[1,3,†]

[1]*Conservation Ecology Center, Smithsonian Conservation Biology Institute, Front Royal, Virginia 22630 USA*
[2]*U.S. Geological Survey, National Research Program – Eastern Branch, Reston, Virginia 20192 USA*
[3]*Center for Tropical Forest Science, Smithsonian Tropical Research Institute, Panama City 9100 Panama*
[4]*Smithsonian National Museum of Natural History, Washington, D.C. 20013 USA*

Citation: Gonzalez-Akre, E., V. Meakem, C.-Y. Eng, A. J. Tepley, N. A. Bourg, W. McShea, S. J. Davies, and K. Anderson-Teixeira. 2016. Patterns of tree mortality in a temperate deciduous forest derived from a large forest dynamics plot. Ecosphere 7(12):e01595. 10.1002/ecs2.1595

Abstract. Tree mortality is one of the most influential drivers of forest dynamics, and characterizing patterns of tree mortality is critical to understanding forest dynamics and ecosystem function in the present era of global change. Here, we use a unique data set of mortality in a temperate deciduous forest to characterize rates and drivers of mortality. At the 25.6-ha Center for Tropical Forest Science—Forest Global Earth Observatory forest dynamics plot at the Smithsonian Conservation Biology Institute (Virginia, USA), we conducted two full tree censuses in 2008 and 2013 and then tracked mortality over the next 2 years (2014 and 2015). Overall, the mortality rate, m, of stems ≥10 cm diameter was 1.3–2.1%/yr. Biomass mortality, M, was 1.9–3.4 $Mg{\cdot}ha^{-1}{\cdot}yr^{-1}$ at the stand level (0.6–1.1%/yr of biomass), less than biomass gains from growth and recruitment, resulting in net live biomass accumulation. Small stems died at the highest rate; however, contributions to M increased toward larger size classes. Most species had $m < 2$%/yr and $M < 0.25$ $Mg{\cdot}ha^{-1}{\cdot}yr^{-1}$ (<3%/yr of biomass), whereas two to four species had anomalously high mortality rates during each census period, accounting for 15–24% of m ($n = 2$, *Cercis canadensis*, *Ulmus* species) and 39–75% of M ($n = 4$ *Quercus* species). Stems that died, whether or not in association with mechanical damage, tended to grow more slowly in preceding years than surviving stems and, for certain shade-intolerant species, tended to be in neighborhoods with higher basal area. These findings show how relatively fine-scale mortality processes contribute to stand-level compositional change and carbon cycling. The mortality patterns reported here will provide a valuable basis for understanding future disturbance events within eastern deciduous forests and for comparing across forest types.

Key words: annual mortality census; Center for Tropical Forest Science—Forest Global Earth Observatory; large forest dynamics plot; temperate broadleaf deciduous forest; tree mortality.

Received 6 May 2016; revised 1 August 2016; accepted 6 October 2016. Corresponding Editor: Debra. P. C. Peters.
Copyright: © 2016 Gonzalez-Akre et al. This is an open access article under the terms of the Creative Commons Attribution License, which permits use, distribution and reproduction in any medium, provided the original work is properly cited.
† **E-mail:** teixeirak@si.edu

Introduction

Tree mortality is one of the most influential drivers of forest dynamics, fueling community change (Manion 1981, Bugmann 2001, Keane et al. 2001) and strongly influencing forest carbon (C) cycles (Malhi et al. 2015, Trumbore et al. 2015). Tree mortality drivers range from fine-scale processes (e.g., competition, wind, pathogens) that typically kill individuals or small groups of trees, to episodic events (e.g., droughts, fires, major storms, pest/pathogen outbreaks) that operate at scales of stands to landscapes. Although extensive mortality events typically draw our attention due to their potential to bring about rapid and dramatic changes in forest composition,

structure, and function (e.g., Campbell et al. 2007, Chambers et al. 2007, Chapin et al. 2008, Kurz et al. 2008, Allen et al. 2010), understanding finer-scale mortality processes is essential to understanding forest responses to gradually changing climatic drivers and in providing a background trend needed to interpret the effects of more extensive, episodic events (e.g., Bennett et al. 2015, Trumbore et al. 2015, Das et al. 2016).

In the current era of global change, changes to tree mortality rates may have dramatic impacts on forests. Increasing mortality rates have been documented in a number of forested regions worldwide (e.g., Phillips et al. 2004, van Mantgem et al. 2009, Peng et al. 2011, Brienen et al. 2015, McDowell et al. 2015, Smith et al. 2015). Such changes may be attributable to climate change and associated increases in disturbances such as droughts, insect outbreaks, and fires (IPCC 2013, Weed et al. 2013, Trenberth et al. 2014, Barbero et al. 2015, McDowell et al. 2015). Elevated tree mortality rates have also been linked to other global change pressures including habitat fragmentation (Mesquita et al. 1999, Laurance et al. 2001), altered atmospheric chemistry including acidic deposition from precipitation (Driscoll et al. 2003, Dietze and Moorcroft 2011), invasive pests and pathogens (Karnosky 1979, Elliott and Swank 2008, Meentemeyer et al. 2008, Flower et al. 2013), and altered faunal communities (Rooney 2001, McShea 2012). As global change pressures continue to intensify, forests worldwide may experience increased mortality, with potentially dramatic consequences for forest diversity and climate feedbacks (e.g., Westerling et al. 2011, McDowell et al. 2015, Trumbore et al. 2015). Understanding these impacts will require improved monitoring, analysis, and modeling of tree mortality, in both the absence of and following major disturbance events (Adams et al. 2010, Dietze and Moorcroft 2011, Hicke et al. 2011, Trumbore et al. 2015).

Although broadleaf deciduous forests of the eastern USA are among the best-studied ecoregions on Earth (Martin et al. 2012), we still have limited understanding of their mortality patterns, particularly at the scale of individual stands. This is because tree mortality typically occurs at a relatively low rate (<2.5%/yr; Lines et al. 2010, Reilly and Spies 2016), thereby requiring that large numbers of trees be monitored continuously to detect mortality rate differences across species, size classes, or environments; to capture rare mortality events; or to detect small variations that may be subtle indicators of important changes (Condit et al. 1995, Wagner et al. 2010, Dietze and Moorcroft 2011, Lutz 2015). Sufficient sample sizes are available at a regional scale from the U.S. Forest Inventory and Analysis program, and have been used to characterize mortality rate variation with tree size, species, and environmental factors (Lines et al. 2010, Dietze and Moorcroft 2011). However, we are unaware of any study in an eastern U.S. forest where mortality was monitored in a single plot large enough to allow characterization of mortality rate variation across species, size classes, or spatial neighborhoods.

Here, we use a unique data set of mortality in a U.S. eastern deciduous forest to characterize the rates and drivers of chronic tree mortality processes. Specifically, we analyze data from four censuses at a large (25.6 ha) forest dynamics plot that is part of the Center for Tropical Forest Science—Forest Global Earth Observatory (CTFS-ForestGEO). CTFS-ForestGEO plots are well suited for monitoring tree mortality, given their large size (2–120 ha; 90% ≥10 ha) and regular tree censuses (typically every 5 years; Anderson-Teixeira et al. 2015*a*, Lutz 2015). With the large sample size afforded by these plots, it is possible to characterize mortality rates by size, species, and microhabitat (Condit et al. 1995, Suresh et al. 2010, Lutz et al. 2014, Larson et al. 2015), which in turn allows isolation of the effects of disturbances (e.g., droughts; Condit et al. 2004, Itoh et al. 2012, Bennett et al. 2015). Using two full censuses spaced 5 years apart in combination with two annual mortality censuses, we characterize mortality rate (m; %/yr) and aboveground biomass mortality rate (M; $Mg{\cdot}ha^{-1}{\cdot}yr^{-1}$) over a 7-year period, quantify contributions of different stem size classes and species, and identify factors associated with tree mortality. These analyses should be valuable for comparison with future mortality trends in this forest and with other forest plots globally.

Methods

Study site

The study was conducted in the CTFS-ForestGEO large forest dynamics plot at the Smithsonian

Conservation Biology Institute (SCBI) in north-central Virginia, USA (38°53′36.6″ N, 78°08′43.4″ W; Bourg et al. 2013, Anderson-Teixeira et al. 2015*a*). This 25.6-ha plot is a mature, mixed deciduous forest that developed following logging and agricultural use in the mid-19th century. The dominant canopy tree species are *Liriodendron tulipifera* L., hickories (*Carya* spp.), oaks (*Quercus* spp.), and *Fraxinus americana* L. Elevation ranges from 273 to 338 m a.s.l. Based on a weather station located just outside the plot, mean annual temperature from 2009 to 2014 was 12.9°C and mean annual precipitation was 1001 mm (Anderson-Teixeira et al. 2015*a*). Weather during the study period (2008–2015) was not strongly anomalous relative to prevailing conditions at nearby weather stations over the most recent two decades (Fig. 1).

Field methods

In 2008, a forest monitoring plot (25.6 ha; 640 × 400 m) was established following standardized protocols of the CTFS-ForestGEO network (Condit 1998). Specifically, the locations of all woody stems ≥1 cm diameter at breast height (*D*) were mapped, tagged, and identified to species, and *D* was measured (Bourg et al. 2013). A second census was conducted in 2013 using the same methodology. Henceforth, we refer to these censuses as "full" censuses (as opposed to mortality censuses, described below). These censuses were conducted between early spring and late fall. Data from these two full censuses are included in analyses presented here and form the foundation for the subsequent annual mortality surveys. Full census data are available through the CTFS-ForestGEO data repository (http://ctfs.si.edu/Public/plotdataaccess/), and 2008 census data are also published in Bourg et al. (2013).

In 2014 and 2015, we conducted tree mortality censuses for the cohort of stems with $D \geq 10$ cm at the time of the last full CTFS-ForestGEO census (2013). We visited every stem above the size threshold that was recorded as alive in the previous year and recorded its present status (live or dead). Stems were categorized as dead if there was no green foliage present at time of the census (during the growing season) and it displayed one or more of the following criteria: bark loose or detached from the bole in multiple locations with no evidence of living cambium underneath, failed development of flower or leaf buds, lack of fine twigs, stem snapped below the crown, tree uprooted, or signs of biotic pests or pathogens (e.g., fungus, insect bore-holes). For dead stems, we measured *D* (2015 only) and registered a number of variables to aid in interpreting the likely agents contributing to mortality (Appendix S1: Table S1), including crown position (sensu Miller et al. 1996), crown condition (sensu Muller-Landau and Dong 2010), liana load (quantified on a five-point categorical scale following Clark and Clark 1992), and potential factors associated with the stem death (FADs; modified from Lutz and Halpern 2006). FADs included mechanical damage (e.g., broken trunk, uprooted tree) and biological damage (e.g., macroscopic fungi or superficial beetle damage; see Appendix S1: Table S1). In 2014, we recorded the presence of these readily observable external conditions but did not attempt thorough identification of damage by pests and pathogens. In 2015, we visually inspected stems for signs of specific identified common pests and pathogens in southeastern US temperate forests (e.g., emerald ash borer—*Agrilus planipennis* Fairmaire (Coleoptera: Buprestidae)—and *Armillaria* root disease). These censuses were completed during the middle and latter part of the growing season (September–October 2014; June–August 2015). Data for these mortality censuses are available in Dryad (Gonzalez-Akre et al. 2016; http://dx.doi.org/10.5061/dryad.v5h24).

Analyses

Calculating annual mortality rate and biomass mortality.—Annual mortality rate (*m*; %/yr) and aboveground biomass mortality (henceforth, "biomass mortality"; *M*; $Mg \cdot ha^{-1} \cdot yr^{-1}$) were calculated for all three census periods (2008–2013, 2013–2014, and 2014–2015) for the entire plot and for stems subsetted by size class or species (detailed below). Following Sheil et al. (1995), *m* was calculated as

$$m = \left[1 - \left(\frac{N_t}{N_0}\right)^{1/t}\right] \times 100 \quad (1)$$

where N_0 is the number of live stems in the first census, and N_t is the number of stems that remained alive in the subsequent census at time *t*, calculated based on exact sample dates. Ninety-five percent confidence intervals (CIs) were determined using the normal approximation

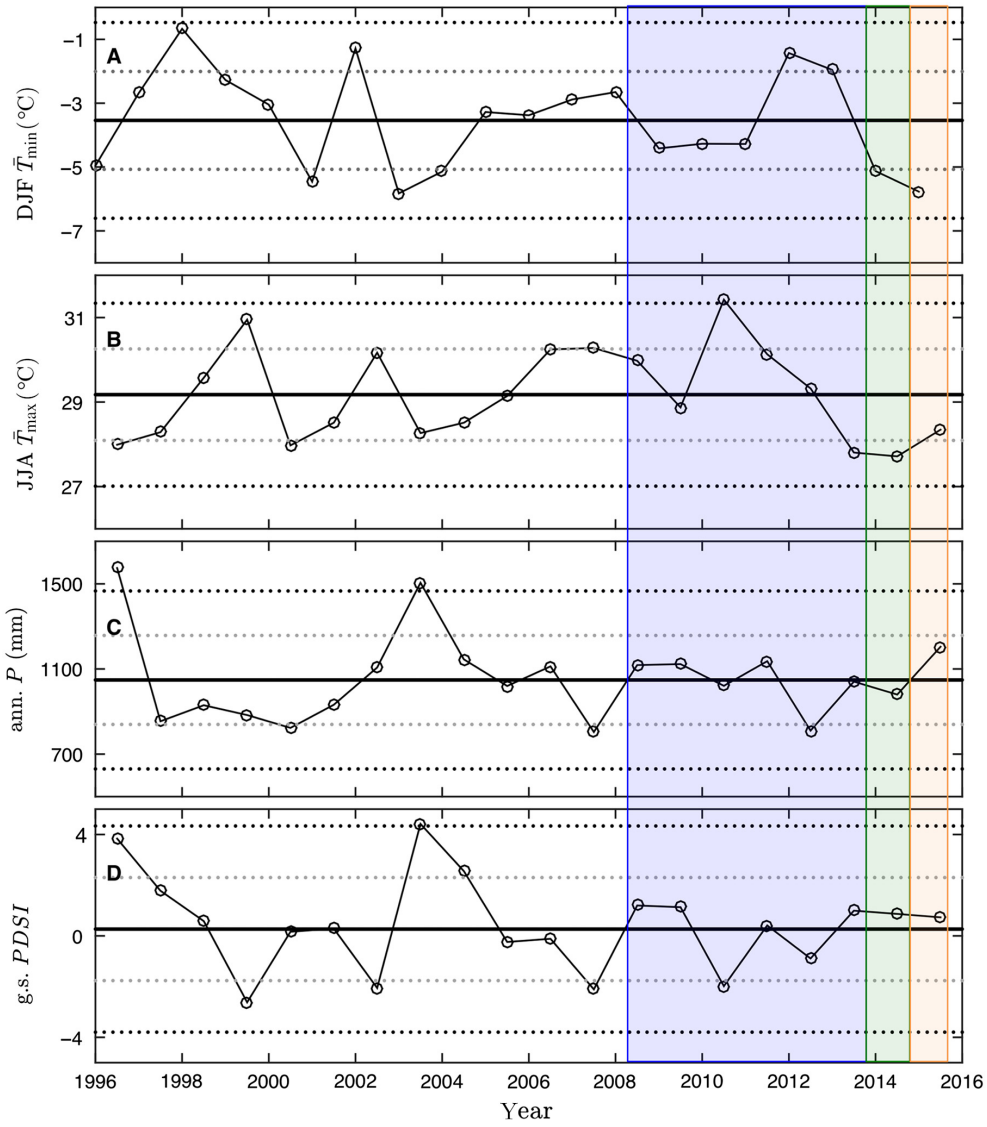


Fig. 1. Smithsonian Conservation Biology Institute mortality census periods in the context of 20 years of history for four climatic variables: (A) mean winter (DJF) minimum temperature (T_{min}), (B) mean summer (JJA) maximum temperature (T_{max}), (C) annual precipitation (P), and (D) average growing season (April–October) Palmer Drought Severity Index (PDSI). Average values are plotted at the center of the 1-year aggregating period: July of the preceding year to June for DJF T_{min} and the calendar year for all others. Solid line indicates 20-year mean; dotted lines indicate ±1 SD (gray) or ±2 SD (black). Censuses periods are shaded with colors corresponding to those used in Figs. 2–4. Data obtained from NOAA's National Climatic Data Center (www.ncdc.noaa.gov/data-access); PDSI values obtained from NOAA's Gridded Climate Divisional Dataset (www.ncdc.noaa.gov/cag/time-series), Front Royal, Virginia; GHCND: USC00443229, November 2015.

to the binomial variance, unless there were five or fewer dead stems, in which case exact binomial probabilities were used (Condit et al. 1995).

Biomass mortality, M, was calculated by summing the aboveground biomass of all stems that died and dividing by plot area. Stem biomass was estimated using local and species-specific

biomass allometries, when possible (Appendix S1: Table S2). Allometric equations were obtained from existing compilations for North America (Jenkins et al. 2004, Chojnacky et al. 2014). For each species, we selected among available allometries in the following order of priority: (1) species-specific allometries > genus-specific allometries > family-specific allometries; (2) proximity to site > regional allometries. When no biomass regressions were found for a particular species ($n = 11$) at any taxonomical level, we used the generalized equation for "mixed woods" in Jenkins et al. (2004). Biomass was calculated based on 2013 D measurements (2008–2013 and 2013–2014 census periods) or on D measurements of dead stems if greater than or equal to the corresponding 2013 measurements (2014–2015 census period). The latter criterion was employed because a loss of bark sometimes resulted in the 2015 D measurement being less than the 2013 measurement. Because the 2013–2014 census period used D measurements from the beginning, as opposed to the end, of the census period, M may be slightly underestimated for this census period.

For cases where multiple stems arise from a common root collar (e.g., *Quercus* spp., *Tilia* sp.) or from the same root system (e.g., *Asimina triloba*), all analyses refer to mortality at the level of individual stems (ramets), as opposed to the whole tree (genet), unless otherwise stated. The majority of stem deaths analyzed here were also tree deaths (91.4% of all deaths of stems with $D \geq 10$ from 2008 to 2015).

Unless stated otherwise, analyses include only stems with $D \geq 10$ cm at the time of the most recent full plot census (2008 or 2013). Note that calculations apply to cohorts of stems based on D in the most recent full tree census (2008 or 2013) and thereby exclude any trees that grew into the 10 cm diameter class thereafter. Because some trees could grow into the 10 cm diameter class and then die before the next five-year census, our results for any census period but the first year following a full census (here, 2013–2014 census period) could underestimate m and M values (Sheil and May 1996, Lewis et al. 2004). An empirical correction proposed for tropical forests suggests that m measured over a 5-year census interval should be increased by ~14% to be comparable to a 1-year census interval (Lewis et al. 2004); however, this correction was not applied here because we would not expect the same correction factor to be appropriate in forests with different stem size distributions or turnover rates.

Role of mortality in biomass change.—To characterize the role of mortality in changes in aboveground live biomass, we calculated aboveground net primary production of stem biomass ($ANPP_{stem}$), recruitment, and M to obtain net biomass change (Δ Biomass = $ANPP_{stem}$ + Recruitment − M; all units $Mg{\cdot}ha^{-1}{\cdot}yr^{-1}$) over the 2008–2013 census period for several size classes based on D in 2008 ($D \geq 1$ cm, <10 cm, 10–30 cm, 30–50 cm, and ≥50 cm). $ANPP_{stem}$ was calculated using allometric relationships (Appendix S1: Table S2) based on the change in D for stems that were alive in both census periods (following variable definition in Anderson-Teixeira et al. 2016). Recruitment was calculated by summing the annual biomass change for stems added to the census in 2013 (i.e., stems that grew into the size class since the 2008 census).

Variation by stem size.—Size-related variation in m and M was analyzed for each census period (2008–2013: ≥1 cm, 2013–2014, and 2014–2015: ≥10 cm) using methodology similar to that of Muller-Landau et al. (2006) for m. Stems were subsetted into log-even bins ($n = 11$ for stems ≥10 cm; 21 bins for stems ≥1 cm), with the final bin expanded to include all stems above its lower diameter cutoff (81 cm), and m, M, and mean initial diameter ($\overline{D_0}$; i.e., D measured at the most recent full CTFS-ForestGEO census) were calculated for each size class. For consistency with previous work representing size scaling of variables that sum, as opposed to average, across size bins (e.g., West et al. 2009, Lutz et al. 2012), total M for each size bin was divided by the width of the size bin (cm). Because the largest size bin was not log-even, it was excluded from the M regressions. Data were ln-transformed for fitting. For both m and M, we fit a linear least squares regression to ln-transformed data, which corresponds to a power function, where a and b are fitted parameters:

$$m \text{ or } M = a\overline{D_0}^{b} \quad (2)$$

For m, we also fit a function that would allow for either a power law or U-shaped fit, both of which have precedent in the literature (Muller-Landau et al. 2006, Coomes and Allen 2007,

Hurst et al. 2011, Anderson-Teixeira et al. 2015*b*). We do not present the results for *U*-shaped fits here because the parameter influencing the *U*-shape was not statistically significant (at $P = 0.05$) and the AICc was higher than that for a model that lacked this parameter (Appendix S1: Table S4). For both m and M, fits were analyzed separately for each census period (stems with $D_0 \geq 10$ cm) and for all stems with $D_0 \geq 1$ cm for the 2008–2013 census period. As in Muller-Landau et al. (2006), 95% CIs were obtained by bootstrapping across 50 × 50 m subplots using 1000 bootstrap replicates.

Variation among species.—To examine variation in mortality among species, we calculated m and M for stems within each species and census period, considering only stems with $D_0 \geq 10$ cm and species with ≥100 individuals above this size threshold. We then characterized the distribution of mortality rates among species, using a one-sample Kolmogorov–Smirnov test to test the null prediction that species mortality rates were normally distributed.

Previous growth rates.—To test whether stem survival or death was related to diameter growth in the preceding years, we compared 2008–2013 growth rates of stems ≥10 cm in the 2013 census that died in 2014 or 2015 with those that lived through 2015. Diameter growth rate (g; mm/yr) was calculated by dividing the change in D by the time elapsed between exact measurement dates during the 2008–2013 interval. We then characterized size-related variation of g for three groups of stems: (1) those that lived through 2015, (2) those that died of biological or unknown causes in 2014 or 2015, and (3) those that died of physical damage in either 2014 or 2015. Data from 2014 and 2015 were combined to increase sample size and because $g - D$ relationships did not vary between years. Stems were inferred to have died from physical damage if they were broken, crushed, uprooted, or struck by lightning. We also conducted the analysis without separating out physical mortality causes. Stems were grouped into the same log-even bins used to characterize scaling of mortality, and mean g ($\overline{g}$) and $\overline{D_0}$ were calculated for each size class. To reduce the impact of outliers on $\overline{g}$, we discarded stems whose growth fell more than three standard deviations above the mean for each size class. Negative outliers were identified using a linear model to estimate the standard deviation of D measurements due to measurement error, and stems were removed when the D measurement in the second census was more than four standard deviations below the first (Muller-Landau et al. 2006). All outliers comprised ~2% of the total stem number. The relationship between $\overline{g}$ and $\overline{D_0}$ was fit to the following equation using linear least squares regression:

$$\bar{g} = k \times \ln\left(\overline{D_0}/D_{\text{ref}}\right) + \overline{g_{\text{ref}}} \quad (3)$$

Here, k is the slope of the relationship, $\overline{g_{\text{ref}}}$ is $\overline{g}$ at a reference diameter, and $D_{\text{ref}} = 50$ cm, included in this equation to facilitate statistical comparison of $\overline{g}$ at a D within the range of stem sizes studied. To allow comparison across the same range of D for each census period, we considered only stems with $10 \leq D_0 < 100$ cm.

Spatial neighborhood analysis.—To assess the degree to which local competition influenced stem mortality and the spatial scale at which those influences were most important, we quantified the basal area within circular neighborhoods of varying radii around each stem recorded (alive or dead) in the 2013 census ($n = 9617$). We then compared the neighborhood basal area between stems that survived through the end of the sample period (2015; $n = 7849$) and those recorded as dead in any of the censuses ($n = 1768$). To conduct these calculations, we first determined the distance from each stem to all other living stems in the plot, limited to stems with $D \geq 10$ cm in 2013. Then, for each focal stem, the basal area of all other living stems was summed over each circular neighborhood with radius increasing from 0 to 20 m in 0.5-m increments. For trees with multiple stems originating from a common root collar, we calculated neighborhood basal area for each stem by excluding the basal area of the focal stem and assigning a distance of 0 m to each of the other stems arising from the same root collar. For trees located <20 m from the edge of the plot, we calculated the neighborhood basal area only over radii up to the distance to the plot boundary. We compared whether neighborhood basal area differed between stems that died and those that survived by conducting a Kruskal–Wallis test for each 0.5-m increment in neighborhood radius. Unlike other point pattern analysis methods that

address only the degree of clustering/dispersion among points or the attraction/repulsion between points of two different types (i.e., the univariate and bivariate forms, respectively, of Ripley's *K* analysis), our analysis allowed us to use basal area within the local neighborhood as a continuous proxy for the competitive pressure faced by the focal stem, and we compared this proxy between living and dead stems across a range of neighborhood radii.

All analyses were run using R version 3.1.3 (R Core Team 2013).

Results

Overall, mortality rates of stems ≥10 cm *D* at the most recent full census were 2.1 (95% CI: 2.0, 2.3), 1.3 (95% CI: 1.1, 1.5), and 1.4%/yr (95% CI: 1.2, 1.8) in the 2008–2013, 2013–2014, and 2014–2015 census periods, respectively (Table 1). Mortality rates of trees (including multi-stem individuals) were similar to stem mortality rates for individuals with main stems ≥10 cm, but lower for smaller stems (Table 1); that is, it was not unusual for a small stem to die while one or larger stems originating from the same root collar remained alive.

Biomass mortality, *M*, for stems ≥10 cm at the time of the preceding full census was 3.4, 1.9, and 2.9 Mg C·ha^{-1}·yr^{-1} for the three census periods (Table 1), which corresponded to 1.1, 0.6, and 0.9%/yr of live biomass, respectively. For the 2008–2013 census period, *M* was less than biomass gain through growth and recruitment for each of several size classes (Fig. 2; Appendix S1: Table S3). For the entire stand (all stems ≥1 cm), $ANPP_{stem}$ was 6.42 Mg·ha^{-1}·yr^{-1}, biomass gain through recruitment was 0.08 Mg·ha^{-1}·yr^{-1}, and *M* was 3.62 Mg·ha^{-1}·yr^{-1}, yielding an annual net biomass gain of 2.88 Mg·ha^{-1}·yr^{-1}.

Mortality for the 2008–2013 census period was concentrated in stems <10 cm (Fig. 3), such that *m* was 6.1%/yr for stems <10 cm compared to 2.1%/yr for stems ≥10 cm, with an overall *m* of 5.2%/yr (Table 1). For all three census periods, *m* declined or had a declining tendency ($b < 0$; Eq. 2) as $\overline{D_0}$ increased from ≥10 cm ($P \leq 0.05$ except for 2014–2015, where $P = 0.06$; Appendix S1: Table S4). For all censuses, there was a tendency toward an increase in *m* in the larger size classes, but it was not statistically significant, likely due to the small sample size of large stems (Appendix S1: Table S4). Despite their lower abundance and lower mortality rates, large stems contributed more to biomass mortality at the ecosystem level (Figs. 2, 3B). *M* increased as a power function (Eq. 2) with $\overline{D_0}$ across the size classes ranging from ≥1 cm for the 2008–2013 period. For stems ≥10 cm, the increase in *M* with $\overline{D_0}$ was significant for the 2008–2013 and 2013–2014 census periods

Table 1. Summary of stand-level mortality during each census period at the SCBI CTFS-ForestGEO plot.

Census period	D_0 (cm)	Level	N_0	*n* died	Mortality rate (*m*; %/yr) (95% CI)	Factors associated with stem mortality (%)†		Aboveground biomass mortality (*M*; Mg·ha^{-1}·yr^{-1})‡		
						Physical damage	Biological/ unknown	Total	Physical damage	Biological/ unknown
2008–2013	≥1	Stems	38,976	8486	5.2 (5.0, 5.3)	–	–	3.6	–	–
		Trees	30,006	5007	3.8 (3.7, 4.0)	–	–	n/a	–	–
	1–10	Stems	30,420	7665	6.1 (5.9, 6.2)	–	–	0.21	–	–
		Trees	21,699	4246	4.6 (4.5, 4.7)	–	–	n/a	–	–
	≥10	Stems	8556	821	2.1 (2.0, 2.3)	–	–	3.4	–	–
		Trees	8307	761	2.0 (1.9, 2.2)	–	–	n/a	–	–
2013–2014	≥10	Stems	8067	127	1.3 (1.1, 1.5)	47	53	1.9	0.62	1.23
		Trees	7882	121	1.2 (1.0, 1.5)	47	53	n/a	n/a	n/a
2014–2015	≥10	Stems	7940	91	1.4 (1.2, 1.8)	34	66	2.9	1.22	1.68
		Trees	7761	87	1.4 (1.1, 1.7)	34	66	n/a	n/a	n/a

Note: CTFS-ForestGEO, Center for Tropical Forest Science—Forest Global Earth Observatory; SCBI, Smithsonian Conservation Biology Institute.

† This is the percentage of mortality events associated with each factor. These were calculated separately for stems and trees, but values were identical to the level of precision presented.

‡ *M* was not calculated at the tree level because, for this ecosystem-level property, it is irrelevant whether dead stems are connected to living stems.

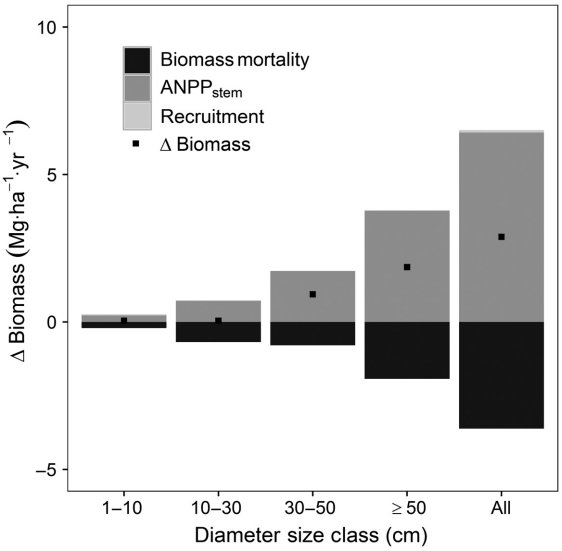


Fig. 2. Net biomass change from 2008 to 2013 as a sum of ANPP$_{stem}$, *M*, and recruitment for all stems ≥1 cm and for four size classes. ANPP$_{stem}$, aboveground net primary production of stem biomass.

(both $P < 0.02$, both $R^2 \geq 0.54$), but not for the 2014–2015 census period ($P = 0.07$, $R^2 = 0.36$; Fig. 3B; Appendix S1: Table S4).

Stem mortality rates varied among species, sometimes significantly so (Fig. 4; Appendix S1: Table S5). Mortality rates for most species with ≥100 stems of $D_0 \geq 10$ cm remained similarly low (i.e., with overlapping 95% CIs) at ≤3.1%/yr in all census intervals. However, two species had $m > 5$%/yr during all three census periods: *Ulmus rubra* ($m = 8.9$–18.6%/yr) and *Cercis canadensis* ($m = 5.2$–6.5%/yr). Biomass mortality was likewise variable among species, being highest among *Quercus* species (Fig. 4B; for all *Quercus* combined, $M = 0.7$–2.2 Mg·ha^{-1}·yr^{-1}), which together comprised 35.7% of total community biomass in 2008 (Appendix S1: Table S3). During each census period, both *m* and *M* had strongly right-skewed distributions (all $P < 0.001$); there were consistently many species with low mortality rates and few species with high mortality (Fig. 4). For both *m* and *M*, the few species with highest mortality rates contributed substantially to total mortality: *U. rubra* and *C. canadensis* together accounted for 15–24% of total *m*, and the four *Quercus* species in the plot together accounted for 39–75% of total *M* (Table 2).

The species with anomalously high mortality rates declined in abundance and community dominance between 2008 and 2013 (Appendix S1: Tables S3 and S5); that is, their high mortality rates were not balanced by high recruitment or ANPP$_{stem}$. Specifically, both of the species with $m > 5$% experienced net declines in abundance (*U. rubra*: −56%; *C. canadensis*: −6%) and biomass (*U. rubra*: −2.35 Mg/ha or −135%; *C. canadensis*: −0.06 Mg/ha or −10%). The genus contributing disproportionately to *M*, *Quercus*, decreased in abundance by 9.6%. *Quercus* increased slightly in biomass (0.9 Mg/ha or 0.8%) but decreased in biomass of stems ≥50 *D* (−0.4 Mg/ha or −0.5%) and proportion of total community biomass (from 35.7% in 2008 to 34.4% in 2013, or −3.6%).

In both annual census periods, 30–50% of both *m* and *M* was associated with physical damage to stems (breakage or uprooting; Table 1). Regardless of whether mortality was associated with physical damage, stems that died had, on average, slower diameter growth between 2008 and 2013 than stems that survived throughout the sampling period (Fig. 5). For all stem sizes, $\overline{g}$ increased with $\overline{D_0}$ (see Eq. 3; all $P \leq 0.007$, all $R^2 \geq 0.57$; Appendix S1: Table S6); however, stems that died of biological or unknown causes in 2013–2014 or 2014–2015 grew more slowly, on average, during the 2008–2013 census interval than stems of the same size that survived through 2015 (Fig. 5). Specifically, $\overline{g_{ref}}$ was significantly higher for stems that lived through 2015 ($\overline{g_{ref}} = 0.40$, 95% CI: 0.37–0.43) than for those that died of biological/ unknown causes ($\overline{g_{ref}} = 0.17$, 95% CI: 0.11–0.22) or were physically damaged ($\overline{g_{ref}} = 0.27$, 95% CI: 0.19–0.35). Similar results were found if causes of mortality, physical, and biological/unknown were combined (Appendix S1: Table S6). The difference tended to be greater for large than for small stems; that is, $\overline{g}$ increased with $\overline{D_0}$ significantly more steeply for stems that lived until 2015 ($k = 0.21$, 95% CI: 0.17–0.25) than for stems that died of biological/unknown causes ($k = 0.10$, 95% CI: 0.04, 0.17), and the slope was intermediate for physically damaged stems ($k = 0.17$, 95% CI: 0.07, 0.27).

Competitive influences, inferred from the basal area within circular neighborhoods surrounding each tree, were not a primary cause of mortality when compiled across all stems in the

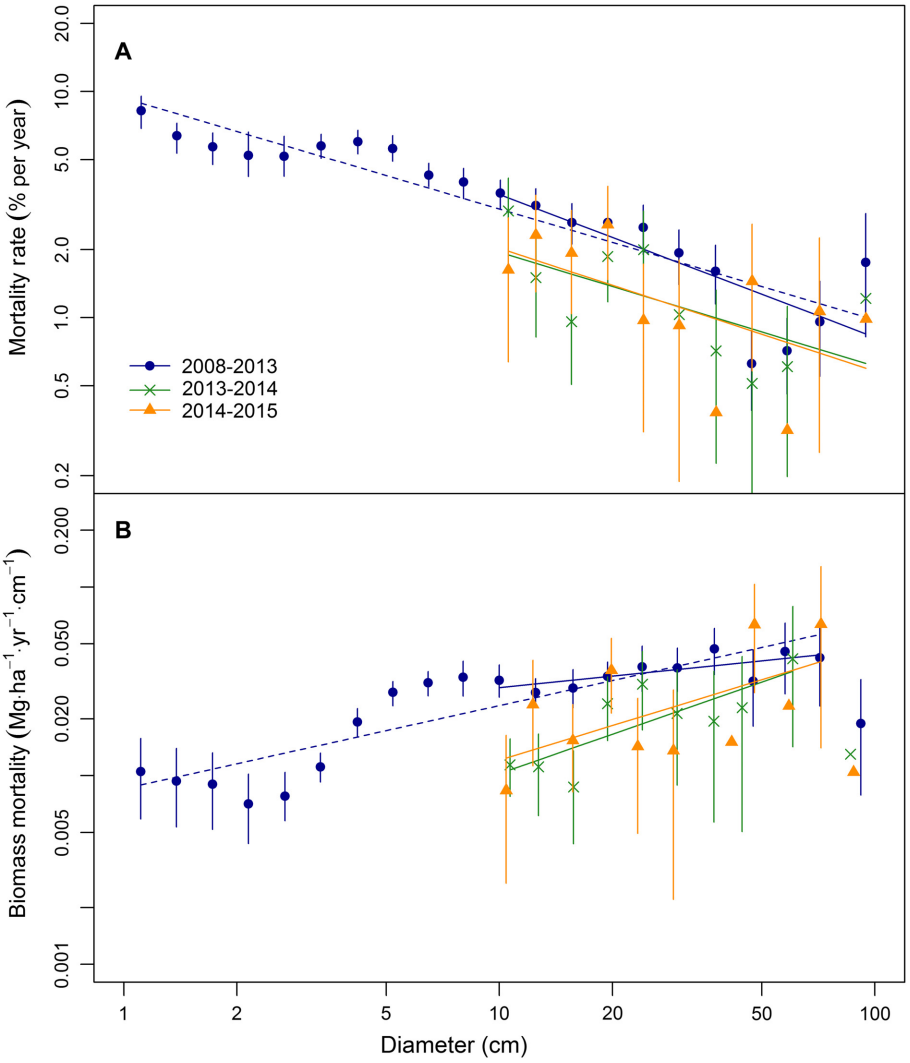


Fig. 3. Size dependence of (A) mortality rate, *m*, and (B) aboveground biomass mortality rate (*M*; Eq. 2) for the three census periods. All stems in the plot are binned into log-even diameter bins. To depict how *M* changes with diameter on a linear scale, the total *M* for each size bin is divided by the width of the size bin (cm). Because the width of the final size bin is not log-even (see *Methods*), this final point is excluded from the regressions. Points represent calculated mortality rate; vertical lines represent 95% CIs based on bootstrapping analysis. Solid lines represent fit for stems >10 cm *D*; dotted lines represent fit for all stems censused. Note logarithmic scales on both axes. Full fit statistics are given in Appendix S1: Table S4.

plot (Fig. 6A). However, certain shade-intolerant species showed a tendency toward higher mortality among individuals surrounded by higher basal area within small neighborhoods. For instance, in the case of *L. tulipifera*, the species with the highest biomass in the plot, neighborhood basal area was significantly higher ($P < 0.05$) at each 0.5-m increment from 1 to 7 m in neighborhood radius surrounding stems that died during the sample period compared with stems that survived (Fig. 6B). Similarly, for *C. canadensis*, a shade-intolerant small-tree species with the second highest mortality rate in the plot, stems that died tended to be surrounded by higher basal area than those that survived (Fig. 6C), but the difference was statistically

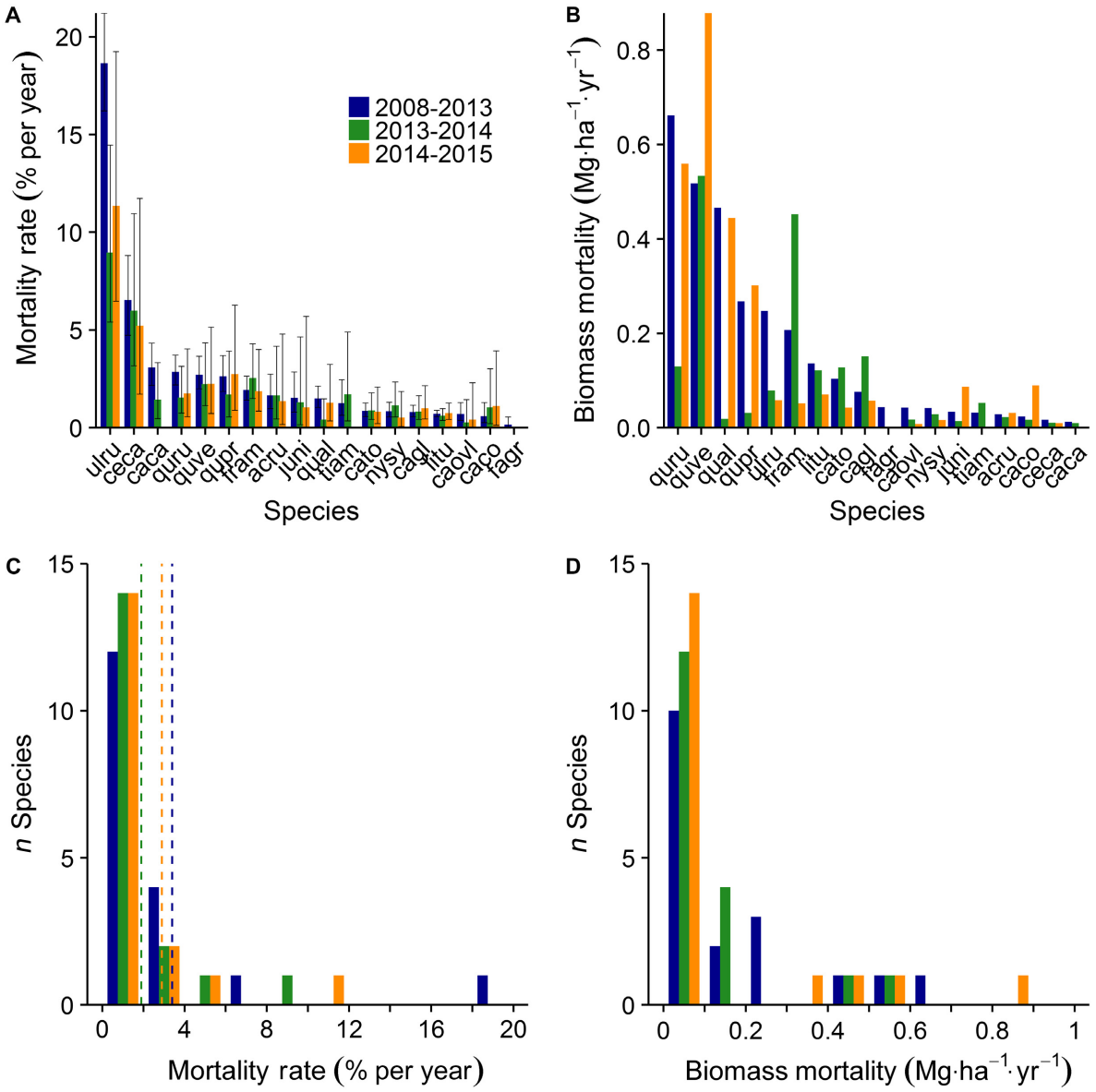


Fig. 4. Mortality rate (A) and aboveground biomass mortality rate (B) by species over the three census periods, along with histograms of these rates (C, D). Included are species with ≥100 stems ≥10 cm *D*. In A and B, species are ranked along the *x*-axes by 2008–2013 rate. Dashed vertical lines in C indicate community-wide mortality rates for stems ≥10 cm *D* for each census period. Species acronyms in A and B as follows: *Acer rubrum* (acru), *Carpinus caroliniana* (caca), *Carya cordiformis* (caco), *Carya glabra* (cagl), *Carya ovalis* (caovl), *Carya tomentosa* (cato), *Cercis canadensis* (ceca), *Fagus grandifolia* (fagr), *Fraxinus americana* (fram), *Juglans nigra* (juni), *Liriodendron tulipifera* (litu), *Nyssa sylvatica* (nysy), *Quercus alba* (qual), *Quercus prinus* (qupr), *Quercus rubra* (quru), *Quercus velutina* (quve), *Tilia americana* (tiam), *Ulmus rubra* (ulru).

significant ($P < 0.05$) only over neighborhood radii from 6.5 to 16.5 m. By contrast, for *Ulmus* spp., whose mortality was driven largely by a pathogen (Dutch elm disease), neighborhood basal area showed minimal difference between stems that died and those that survived throughout the sample period (Fig. 6D). In fact, surviving *Ulmus* stems had significantly higher

Table 2. Comparison of *m* and *M* values including and excluding the species with the highest mortality rates (*Ulmus rubra* and *Cercis canadensis*) and highest *M* values (*Quercus* ssp: *Q. alba*, *Q. rubra*, *Q. velutina*, *Q. prinus*).

		Stem mortality rate (*m*; %/yr)		Aboveground biomass mortality (*M*; $Mg \cdot ha^{-1} \cdot yr^{-1}$)	
Census period	*D*	Total (95% CI)	*U. rubra* and *C. canadensis* excluded (95% CI)	Total	*Quercus* spp. excluded
2008–2013	≥10 cm	2.12 (1.98, 2.27)	1.61 (1.49, 1.75)	3.41	1.43
2013–2014	≥10 cm	1.26 (1.06, 1.50)	1.06 (0.879, 1.29)	1.86	1.14
2014–2015	≥10 cm	1.44 (1.18, 1.77)	1.23 (0.983, 1.54)	2.90	0.72

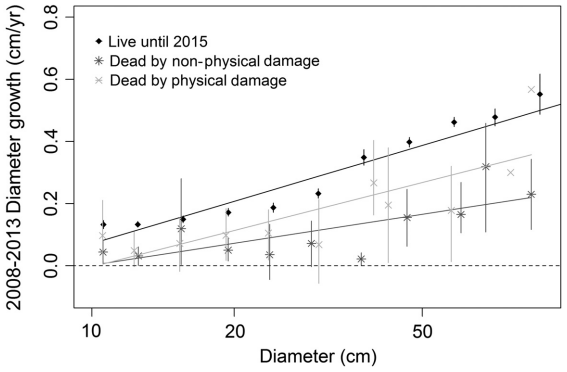


Fig. 5. Five-year census (2008–2013) growth rate as a function of *D* (averaged by size class) for stems that lived through 2015, those that died of biological or unknown causes, and those showing physical damage. Size range starts at *D* = 10 cm and range through the largest size bin with stem deaths in 2014 and 2015 (81–90 cm *D*).

neighborhood basal area than stems that died at neighborhood radii of 3.5 and 4.5–6.0 m ($P < 0.05$).

Discussion

As a whole, the forest community experienced modest rates of tree mortality during the study period. During the interval with highest annual mortality rate (2008–2013), *M* remained less than $ANPP_{stem}$ in all stem size classes, resulting in net live biomass gain (Fig. 2), which is typical of maturing secondary forests in the region (e.g., Barford et al. 2001, Lichstein et al. 2009). While neither static nor invariant, the mortality patterns observed here—including size–mortality relationships (Fig. 3), right-skewed distributions of mortality rates (Fig. 4), slow diameter growth prior to mortality (Fig. 5), and competition-related influences on mortality of certain shade-intolerant species (Fig. 6)—were likely driven primarily by mechanisms that are common in many forest communities.

Whereas smaller stems had higher mortality rates, larger stems contributed more to ecosystem-level biomass mortality (Figs. 2, 3). The observed decline in *m* with *D* (Fig. 3A) is typical in mature secondary or old-growth forests worldwide (Muller-Landau et al. 2006, Anderson-Teixeira et al. 2015*b*) and is typically attributed to asymmetric competition for light or other resources (Coomes et al. 2003, Coomes and Allen 2007, West et al. 2009, Ruiz-Benito et al. 2013). The observed tendency for *m* to increase above $D \approx 50$ cm (Fig. 3A), although not significant, is consistent with observations of *U*-shaped mortality patterns by other studies (Coomes and Allen 2007, Lines et al. 2010, Hurst et al. 2011) and may reflect relatively greater influence of exogenous disturbances on the mortality of dominant canopy trees (Coomes et al. 2003). These larger stems, albeit lower in abundance (Anderson-Teixeira et al. 2015*b*) and having relatively low *m* (Fig. 3A), contributed disproportionately to biomass mortality at the ecosystem level (Figs. 2, 3B). To the extent that this holds true for other forests, understanding mortality rates and drivers of the largest trees—and their sensitivity to global change (e.g., drought; Bennett et al. 2015)—will be particularly important for understanding forest C cycling and feedbacks to climate change.

Whereas most species had relatively low *m* and *M*, there were two to four species in each census period with anomalously high mortality rates (Fig. 4), all of which appear to have been affected by species-specific pests or pathogens. *Ulmus rubra* had the highest mortality rate in all three census periods, and it was likely affected by Dutch elm disease (we recorded diagnostic beetle

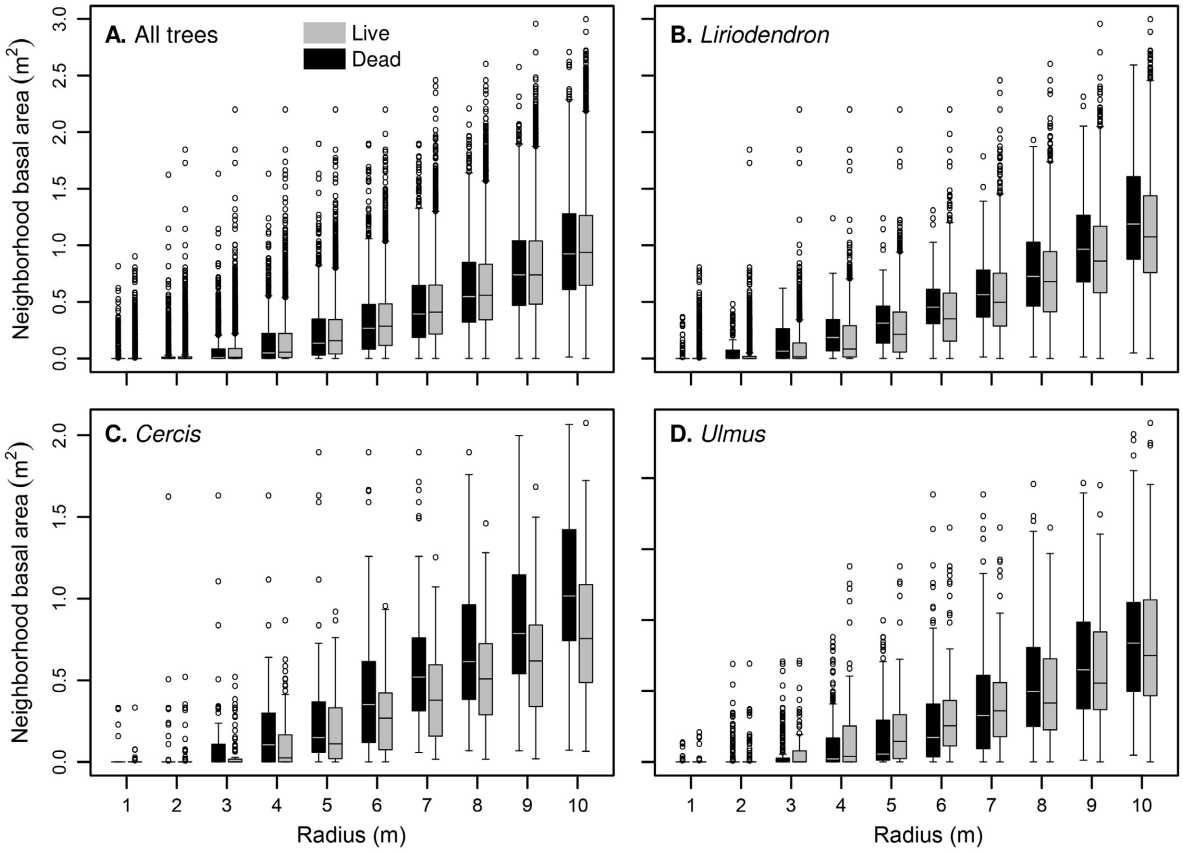


Fig. 6. Influences of local competition on stem mortality inferred from the basal area within circular neighborhoods surrounding each stem ≥10 cm *D* at the SCBI CTFS-ForestGEO plot. Shown are comparisons of basal area within neighborhoods of increasing radius surrounding stems that died between 2008 and 2015 and those that survived and those for the entire study period. Boxplots are presented for visualization purposes only; statistical differences reported in the text were determined using a Kruskal–Wallis (rank-based nonparametric) test on 0.5 m radius bins. Analyses are presented for the following taxa: (A) all species combined (n = 1768 dead; 7849 survivors); (B) *Liriodendron tulipifera*, the most abundant canopy species (n = 129 dead; 2190 survivors); (C) *Cercis canadensis*, the species with the second highest m (n = 55 dead, 114 survivors); and (D) the genus *Ulmus* (*U. americana* and *U. rubra*), which had the highest m (n = 188 dead, 325 survivors). CTFS-ForestGEO, Center for Tropical Forest Science—Forest Global Earth Observatory; SCBI, Smithsonian Conservation Biology Institute.

feeding galleries on numerous dead stems), which has severely reduced the lifespan of *Ulmus* trees throughout US Eastern forests (Smith et al. 2009). The lack of difference in neighborhood basal area surrounding *Ulmus* stems that died and those that survived throughout the sampling period (Fig. 6D) is also consistent with mortality driven primarily by a pathogen rather than competition with surrounding trees. Likewise, *Cercis canadensis* is known to be severely affected by *Botryosphaeria ribis* cankers in the region (Bush 2009, Brakie 2010). Our finding that mortality rates were higher among individuals growing in neighborhoods of higher basal area (Fig. 6C) suggests that competition with neighboring trees may exacerbate the effects of *Botryosphaeria* cankers on *C. canadensis* to a greater degree than local competition intensifies the effects of Dutch elm disease on elm trees. The genus that contributed disproportionately to *M*, *Quercus*, comprised over one-third of the plot biomass and tended to have relatively high m (Fig. 4; Appendix S1: Table S5). *Quercus* is subject to oak decline throughout the region (Oak et al. 2016), and signs of oak decline

were observed on many of the *Quercus* trees that died (e.g., progressive crown die-back, insect exit holes diagnostic of *Agrilus bilineatus*). Importantly, these few species contributed disproportionally to community-wide mortality, with *U. rubra* and *C. canadensis* accounting for up to 24% of *m* and the *Quercus* species accounting for up to 75% of *M* (Table 2). If the pattern observed here proves general—that there is commonly a small minority of species suffering anomalously high mortality at any given time—detecting, characterizing, and modeling their mortality will be critical to understanding mortality rates, drivers, and their consequences in forests composition.

For the remainder of species, mortality appears to have been driven by a mix of mechanical damage and environmental or biotic stressors. The 2014 and 2015 censuses, which recorded factors associated with death, provide some insight into the mechanisms of mortality. Mechanical damage, such as uprooting or stem breakage, was associated with ~40% of the tree deaths between 2013 and 2015 (Table 1). Interestingly, the stems whose mortality was associated with mechanical damage exhibited a tendency for slower growth compared with surviving stems during the years prior to their mortality (Fig. 5). This is consistent with the concept that tree mortality is often driven by multiple interacting factors (Franklin et al. 1987) and suggests that these stems may have been weakened by one or more stress agents in the years preceding their death (e.g., root rot preceding uprooting).

Nonmechanical drivers of mortality—including climatic stress, competition, and infection by pests/pathogens—are more challenging to identify. Our results indicate notably slower growth prior to mortality among the stems that died between 2013 and 2015 and lacked evidence of physical damage (Fig. 5). This finding, while consistent with previous studies showing that slower-growing stems are often at higher risk of mortality and that stems commonly exhibit a slowdown in growth rate prior to death (van Mantgem et al. 2003, Chao et al. 2008, Hereş et al. 2012), does not provide proximate causes of mortality. Our results neither support nor reject climatic variation as an important mortality agent during our census period. The 2008–2013 census interval, which had the highest average annual mortality rate with or without the two species with highest *m* (Tables 1, 2) included some potentially stressful climatic periods: a summer (2010) that was unusually warm (JJA T_{max} > mean + 2 SD) and dry (g.s. PDSI < mean − 1 SD), a year with unusually low rainfall (2012; annual precipitation <mean − 1 SD), and two unusually warm winters (2012 and 2013; DJF T_{min} < mean − 1 SD). This census interval also included an anomalous heavy snowstorm in October 2011, which caused substantial crown damage/breakage. However, a 5-year census is not sufficient to resolve whether any of these affected mortality rate, and the 2013 census protocol did not record factors associated with mortality. The two annual census periods were unlikely to have been climatically stressful to trees, with average or unusually cool temperatures, near-average precipitation, and near-average growing season PDSI (Fig. 1).

When considered irrespective of species, the fact that neighborhood basal area was similar for trees that lived and those that died indicates that competition was not the dominant driver of mortality (Fig. 6A). Rather, this lack of neighborhood effects may be characteristic of mid- to late successional forests where dominant canopy trees are more likely to be killed by wind or biotic agents (pests or pathogens) than competition with other trees (Franklin et al. 2002). However, when considered by species, some shade-intolerant species had higher mortality rates in more crowded neighborhoods (Fig. 6B, C). For instance, in the case of *L. tulipifera*, which dominates the upper canopy, stems that died tended to be surrounded by higher basal area over small neighborhoods (1–7 m radius; Fig. 6B) than those that survived, suggesting that this species faces some degree of competition with neighboring trees. Similarly, as discussed above, our finding that *C. canadensis* stems that died tended to be surrounded by higher basal area within relatively small neighborhoods (6.5–16.5 m radius) may indicate that competition of this understory tree species with neighboring stems exacerbates the effects of *Botryosphaeria* cankers.

In contrast to the relatively low mortality rates observed during our study period, larger, episodic disturbance events that strongly affect large trees or dominant species may result in substantively different mortality patterns (Reilly and Spies 2016). For instance, the recent arrival of emerald ash borer (first recorded in the plot in the

summer of 2015) is expected to cause very high mortality of the three ash species in our plot (*Fraxinus americana*, *F. nigra*, and *F. pennsylvanica*; Flower et al. 2013), which comprise an important component of the canopy. The patterns reported here will provide a valuable contrast for understanding the impact of such future disturbance events. Considering the threat of global change-driven increases in tree mortality in forests worldwide (Runkle 2000, Harcombe et al. 2002, van Mantgem et al. 2009, Allen et al. 2010, McDowell et al. 2015), there is strong need for long-term tree mortality studies (Adams et al. 2010, Dietze and Moorcroft 2011, Hicke et al. 2011, Trumbore et al. 2015). Widespread application of annual tree mortality surveys on large forest dynamics plots will provide greater insights on the annual variability of forest structural and compositional changes due to tree loss associated with anthropogenic, ecological, or climatic disturbances.

Acknowledgments

We thank Valentine Hermann, Maria Wang, Gabriela Reyes, Haley Overstreet, Maryam Sedaghatpour, and Romaric Moncrieffe for assisting with mortality censuses and Helene Muller-Landau for the use of her R scripts. Funds for the full tree censuses were provided by the Smithsonian Institution Center for Tropical Forest Science—Forest Global Earth Observatory (CTFS-ForestGEO). Annual mortality censuses and the analyses presented here were funded by a Smithsonian Competitive Grants Program in Science award to KAT. CYE received support from the Mary Jean Hale Fund. SJD received support from the Next Generation Ecosystem Experiment (NGEE) Tropics project.

Literature Cited

Adams, H. D., A. K. Macalady, D. D. Breshears, C. D. Allen, N. L. Stephenson, S. R. Saleska, T. E. Huxman, and N. McDowell. 2010. Climate-induced tree mortality: earth system consequences. Eos, Transactions, American Geophysical Union 91:153–154.

Allen, C. D., et al. 2010. A global overview of drought and heat-induced tree mortality reveals emerging climate change risks for forests. Forest Ecology and Management 259:660–684.

Anderson-Teixeira, K. J., et al. 2015*a*. CTFS-ForestGEO: a worldwide network monitoring forests in an era of global change. Global Change Biology 21:528–549.

Anderson-Teixeira, K. J., et al. 2015*b*. Size-related scaling of tree form and function in a mixed-age forest. Functional Ecology 29:1587–1602.

Anderson-Teixeira, K. J., M. M. H. Wang, J. C. McGarvey, and D. S. LeBauer. 2016. Carbon dynamics of mature and regrowth tropical forests derived from a pantropical database (TropForC-db). Global Change Biology 22:1690–1709.

Barbero, R., J. T. Abatzoglou, N. K. Larkin, C. A. Kolden, and B. Stocks. 2015. Climate change presents increased potential for very large fires in the contiguous United States. International Journal of Wildland Fire 24:892–899.

Barford, C. C., et al. 2001. Factors controlling long- and short-term sequestration of atmospheric CO_2 in a mid-latitude forest. Science 294:1688–1691.

Bennett, A. C., N. G. McDowell, C. D. Allen, and K. J. Anderson-Teixeira. 2015. Larger trees suffer most during drought in forests worldwide. Nature Plants 1:15139.

Bourg, N. A., W. J. McShea, J. R. Thompson, J. C. McGarvey, and X. Shen. 2013. Initial census, woody seedling, seed rain, and stand structure data for the SCBI SIGEO Large Forest Dynamics Plot. Ecology 94:2111–2112.

Brakie, M. 2010. Plant fact sheet for eastern redbud (*Cercis canadensis*). USDA-Natural Resources Conservation Service, East Texas Plant Materials Center, Nacogdoches, Texas, USA.

Brienen, R. J. W., et al. 2015. Long-term decline of the Amazon carbon sink. Nature 519:344–348.

Bugmann, H. 2001. A review of forest gap models. Climatic Change 51:259–305.

Bush, E. A. 2009. Botryosphaeria canker and dieback of trees and shrubs in the landscape. Virginia Cooperative Extension, Publication 50–726. College of Agriculture and Life Sciences, Virginia Polytechnic Institute, Blacksburg, Virginia, USA.

Campbell, J., D. Donato, D. Azuma, and B. Law. 2007. Pyrogenic carbon emission from a large wildfire in Oregon, United States. Journal of Geophysical Research: Biogeosciences 112:G04014.

Chambers, J. Q., J. I. Fisher, H. Zeng, E. L. Chapman, D. B. Baker, and G. C. Hurtt. 2007. Hurricane Katrina's carbon footprint on U.S. Gulf Coast forests. Science 318:1107.

Chao, K.-J., O. L. Phillips, E. Gloor, A. Monteagudo, A. Torres-Lezama, and R. V. Martínez. 2008. Growth and wood density predict tree mortality in Amazon forests. Journal of Ecology 96:281–292.

Chapin, F. I., J. Randerson, A. McGuire, J. Foley, and C. Field. 2008. Changing feedbacks in the climate-biosphere system. Frontiers in Ecology and the Environment 6:313–320.

Chojnacky, D. C., L. S. Heath, and J. C. Jenkins. 2014. Updated generalized biomass equations for North American tree species. Forestry 87:129–151.

Clark, D. A., and D. B. Clark. 1992. Life history diversity of canopy and emergent trees in a Neotropical rain forest. Ecological Monographs 62:315–344.

Condit, R. 1998. Tropical forest census plots: methods and results from Barro Colorado Island, Panama, and a comparison with other plots. Springer, Berlin, Germany.

Condit, R., S. Aguilar, A. Hernandez, R. Perez, S. Lao, G. Angehr, S. P. Hubbell, and R. B. Foster. 2004. Tropical forest dynamics across a rainfall gradient and the impact of an El Nino dry season. Journal of Tropical Ecology 20:51–72.

Condit, R., S. P. Hubbell, and R. B. Foster. 1995. Mortality rates of 205 Neotropical tree and shrub species and the impact of a severe drought. Ecological Monographs 65:419.

Coomes, D. A., and R. B. Allen. 2007. Mortality and tree-size distributions in natural mixed-age forests. Journal of Ecology 95:27–40.

Coomes, D., R. Duncan, R. Allen, and J. Truscott. 2003. Disturbances prevent stem size-density distributions in natural forests from following scaling relationships. Ecology Letters 6:980–989.

Das, A. J., N. L. Stephenson, and K. P. Davis. 2016. Why do trees die? Characterizing the drivers of background tree mortality. Ecology 97:2616–2627.

Dietze, M. C., and P. R. Moorcroft. 2011. Tree mortality in the eastern and central United States: patterns and drivers. Global Change Biology 17: 3312–3326.

Driscoll, C. T., K. M. Driscoll, M. J. Mitchell, and D. J. Raynal. 2003. Effects of acidic deposition on forest and aquatic ecosystems in New York State. Environmental Pollution 123:327–336.

Elliott, K. J., and W. T. Swank. 2008. Long-term changes in forest composition and diversity following early logging (1919–1923) and the decline of American chestnut (*Castanea dentata*). Plant Ecology 197:155–172.

Flower, C. E., K. S. Knight, and M. A. Gonzalez-Meler. 2013. Impacts of the emerald ash borer (*Agrilus planipennis Fairmaire*) induced ash (*Fraxinus* spp.) mortality on forest carbon cycling and successional dynamics in the eastern United States. Biological Invasions 15:931–944.

Franklin, J. F., H. H. Shugart, and M. E. Harmon. 1987. Tree death as an ecological process. BioScience 37:550–556.

Franklin, J. F., et al. 2002. Disturbances and structural development of natural forest ecosystems with silvicultural implications, using Douglas-fir forests as an example. Forest Ecology and Management 155:399–423.

Gonzalez-Akre, E. B., V. Meakem, C. Y. Eng, A. J. Tepley, N. A. Bourg, W. J. McShea, S. J. Davies, and K. J. Anderson-Teixeira. 2016. Data from: Patterns of tree mortality in a temperate deciduous forest derived from a large forest dynamics plot. Dryad Digital Repository. http://dx.doi.org/10.5061/dryad.v5h24

Harcombe, P. A., C. J. Bill, M. Fulton, J. S. Glitzenstein, P. L. Marks, and I. S. Elsik. 2002. Stand dynamics over 18 years in a southern mixed hardwood forest, Texas, USA. Journal of Ecology 90:947–957.

Hereş, A.-M., J. Martínez-Vilalta, and B. C. López. 2012. Growth patterns in relation to drought-induced mortality at two Scots pine (*Pinus sylvestris* L.) sites in NE Iberian Peninsula. Trees 26:621–630.

Hicke, J. A., et al. 2011. Effects of biotic disturbances on forest carbon cycling in the United States and Canada. Global Change Biology 18:7–34.

Hurst, J. M., R. B. Allen, D. A. Coomes, and R. P. Duncan. 2011. Size-specific tree mortality varies with neighbourhood crowding and disturbance in a Montane Nothofagus forest. PLoS ONE 6:e26670.

IPCC. 2013. Climate change 2013: the physical science basis. Pages 1535 *in* T. F. Stocker, D. Quin, G.-K. Plattner, M. Tignor, S. K. Allen, J. Boschung, A. Nauels, Y. Xia, V. Bex, and P. M. Midgley, editors. Contribution of Working Group I to the Fifth Assessment Report of the Intergovernmental Panel on Climate Change. Cambridge University Press, Cambridge, UK and New York, New York, USA.

Itoh, A., S. Nanami, T. Harata, T. Ohkubo, S. Tan, L. Chong, S. Davies, and T. Yamakura. 2012. The effect of habitat association and edaphic conditions on tree mortality during El Niño-induced drought in a Bornean dipterocarp forest. Biotropica 44:606–617.

Jenkins, J. C., D. C. Chojnacky, L. S. Heath, and R. A. Birdsey. 2004. Comprehensive database of diameter-based biomass regressions for North American tree species. Gen. Tech. Rep. NE-319. U.S. Department of Agriculture, Forest Service, Northeastern Research Station, Newtown Square, Pennsylvania, USA. 45 pp.

Karnosky, D. F. 1979. Dutch Elm Disease: a review of the history, environmental implications, control, and research needs. Environmental Conservation 6:311.

Keane, R. E., M. Austin, C. Field, A. Huth, M. J. Lexer, D. Peters, A. Solomon, and P. Wyckoff. 2001. Tree mortality in gap models: application to climate change. Climatic Change 51:509–540.

Kurz, W. A., C. C. Dymond, G. Stinson, G. J. Rampley, E. T. Neilson, A. L. Carroll, T. Ebata, and

L. Safranyik. 2008. Mountain pine beetle and forest carbon feedback to climate change. Nature 452:987.

Larson, A. J., J. A. Lutz, D. C. Donato, J. A. Freund, M. E. Swanson, J. HilleRisLambers, D. G. Sprugel, and J. F. Franklin. 2015. Spatial aspects of tree mortality strongly differ between young and old-growth forests. Ecology 96:2855–2861.

Laurance, W. F., G. B. Williamson, P. Delamonica, A. Oliveira, T. E. Lovejoy, C. Gascon, and L. Pohl. 2001. Effects of a strong drought on Amazonian forest fragments and edges. Journal of Tropical Ecology 17:771–785.

Lewis, S. L., et al. 2004. Tropical forest tree mortality, recruitment and turnover rates: calculation, interpretation and comparison when census intervals vary. Journal of Ecology 92:929–944.

Lichstein, J. W., C. Wirth, H. S. Horn, and S. W. Pacala. 2009. Biomass Chronosequences of United States Forests: implications for carbon storage and forest management. Pages 301–341 *in* C. Wirth, G. Gleixner, and M. Heimann, editors. Old-growth forests. Springer, Berlin, Heidelberg, Germany.

Lines, E. R., D. A. Coomes, and D. W. Purves. 2010. Influences of forest structure, climate and species composition on tree mortality across the eastern US. PLoS ONE 5:e13212.

Lutz, J. A. 2015. The evolution of long-term data for forestry: large temperate research plots in an era of global change. Northwest Science 89:255–269.

Lutz, J. A., and C. B. Halpern. 2006. Tree mortality during early forest development: a long-term study of rates, causes, and consequences. Ecological Monographs 76:257–275.

Lutz, J. A., A. J. Larson, T. J. Furniss, D. C. Donato, J. A. Freund, M. E. Swanson, K. J. Bible, J. Chen, and J. F. Franklin. 2014. Spatially nonrandom tree mortality and ingrowth maintain equilibrium pattern in an old-growth Pseudotsuga-Tsuga forest. Ecology 95:2047–2054.

Lutz, J. A., A. J. Larson, M. E. Swanson, and J. A. Freund. 2012. Ecological importance of large-diameter trees in a temperate mixed-conifer forest. PLoS ONE 7:e36131.

Malhi, Y., et al. 2015. The linkages between photosynthesis, productivity, growth and biomass in lowland Amazonian forests. Global Change Biology 21:2283–2295.

Manion, P. D. 1981. Tree disease concepts. Prentice-Hall, Englewood Cliffs, New Jersey, USA.

Martin, L. J., B. Blossey, and E. Ellis. 2012. Mapping where ecologists work: biases in the global distribution of terrestrial ecological observations. Frontiers in Ecology and the Environment 10: 195–201.

McDowell, N. G., et al. 2015. Multi-scale predictions of massive conifer mortality due to chronic temperature rise. Nature Climate Change 6:295–300.

McShea, W. J. 2012. Ecology and management of white-tailed deer in a changing world: deer and eastern forests. Annals of the New York Academy of Sciences 1249:45–56.

Meentemeyer, R. K., N. E. Rank, D. A. Shoemaker, C. B. Oneal, A. C. Wickland, K. M. Frangioso, and D. M. Rizzo. 2008. Impact of sudden oak death on tree mortality in the Big Sur ecoregion of California. Biological Invasions 10:1243–1255.

Mesquita, R. C. G., P. Delamônica, and W. F. Laurance. 1999. Effect of surrounding vegetation on edge-related tree mortality in Amazonian forest fragments. Biological Conservation 91:129–134.

Miller, P. R., K. W. Stolte, D. M. Duriscoe, and J. Pronos (Technical Coordinators). 1996. Evaluating ozone air pollution effects on pines in the western United States. Gen. Tech. Rep. PSW–GTR–155. U.S. Department of Agriculture, Forest Service, Pacific Southwest Research Station, Albany, California, USA. 79 pp.

Muller-Landau, H. C., et al. 2006. Testing metabolic ecology theory for allometric scaling of tree size, growth and mortality in tropical forests. Ecology Letters 9:575–588.

Muller-Landau, H. C., and S. X. Dong. 2010. Metal Band Dendrometer Protocol: CTFS Global Forest Carbon Research Initiative. http://www.ctfs.si.edu/data///documents/Metal_Band_Dendrometer_Protocol_20100330.pdf

Oak, S. W., M. A. Spetich, and R. S. Morin. 2016. Oak decline in central hardwood forests: frequency, spatial extent, and scale. Pages 49–71 *in* C. H. Greenberg and B. S. Collins, editors. Natural disturbances and historic range of variation. Springer International Publishing, Switzerland.

Peng, C., Z. Ma, X. Lei, Q. Zhu, H. Chen, W. Wang, S. Liu, W. Li, X. Fang, and X. Zhou. 2011. A drought-induced pervasive increase in tree mortality across Canada's boreal forests. Nature Climate Change 1:467–471.

Phillips, O. L., et al. 2004. Pattern and process in Amazon tree turnover, 1976–2001. Philosophical Transactions of the Royal Society of London Series B: Biological Sciences 359:381–407.

R Core Team. 2013. R: a language and environment for statistical computing. R Foundation for Statistical Computing, Vienna, Austria. http://www.R-project.org/

Reilly, M. J., and T. A. Spies. 2016. Disturbance, tree mortality, and implications for contemporary regional forest change in the Pacific Northwest. Forest Ecology and Management 374:102–110.

Rooney, T. P. 2001. Deer impacts on forest ecosystems: a North American perspective. Forestry 74: 201–208.

Ruiz-Benito, P., E. R. Lines, L. Gómez-Aparicio, M. A. Zavala, and D. A. Coomes. 2013. Patterns and drivers of tree mortality in Iberian forests: climatic effects are modified by competition. PLoS ONE 8: e56843.

Runkle, J. R. 2000. Canopy tree cover in old-growth mesic forests of eastern North America. Ecology 81:554–567.

Sheil, D., D. F. R. P. Burslem, and D. Alder. 1995. The interpretation and misinterpretation of mortality rate measures. Journal of Ecology 83:331–333.

Sheil, D., and R. M. May. 1996. Mortality and recruitment rate evaluations in heterogeneous tropical forests. Journal of Ecology 84:91–100.

Smith, W. D., P. D. Miles, C. H. Perry, and S. A. Pugh. 2009. Forest Resources of the United States, 2007. Gen. Tech. Rep. WO-78. U.S. Department of Agriculture, Forest Service, Washington Office, Washington, D.C., USA.

Smith, J. M., J. Paritsis, T. T. Veblen, and T. B. Chapman. 2015. Permanent forest plots show accelerating tree mortality in subalpine forests of the Colorado Front Range from 1982 to 2013. Forest Ecology and Management 341:8–17.

Suresh, H. S., H. S. Dattaraja, and R. Sukumar. 2010. Relationship between annual rainfall and tree mortality in a tropical dry forest: results of a 19-year study at Mudumalai, southern India. Forest Ecology and Management 259:762–769.

Trenberth, K. E., A. Dai, G. van der Schrier, P. D. Jones, J. Barichivich, K. R. Briffa, and J. Sheffield. 2014. Global warming and changes in drought. Nature Climate Change 4:17–22.

Trumbore, S., P. Brando, and H. Hartmann. 2015. Forest health and global change. Science 349:814–818.

van Mantgem, P. J., et al. 2009. Widespread increase of tree mortality rates in the western United States. Science 323:521–524.

van Mantgem, P. J., N. L. Stephenson, L. S. Mutch, V. G. Johnson, A. M. Esperanza, and D. J. Parsons. 2003. Growth rate predicts mortality of Abies concolor in both burned and unburned stands. Canadian Journal of Forest Research 33:1029–1038.

Wagner, F., E. Rutishauser, L. Blanc, and B. Herault. 2010. Effects of plot size and census interval on descriptors of forest structure and dynamics. Biotropica 42:664–671.

Weed, A. S., M. P. Ayres, and J. Hicke. 2013. Consequences of climate change for biotic disturbances in North American forests. Ecological Monographs 83:441–470.

West, G. B., B. J. Enquist, and J. H. Brown. 2009. A general quantitative theory of forest structure and dynamics. Proceedings of the National Academy of Sciences USA 106:7040–7045.

Westerling, A. L., M. G. Turner, E. A. H. Smithwick, W. H. Romme, and M. G. Ryan. 2011. Continued warming could transform Greater Yellowstone fire regimes by mid-21st century. Proceedings of the National Academy of Sciences USA 108: 13165–13170.

Supporting Information

Additional Supporting Information may be found online at: http://onlinelibrary.wiley.com/doi/10.1002/ecs2.1595/full